

# Study of $K^-$ absorption at rest in nuclei followed by $p\Lambda$ emission\*

Grishma Mehta Pandejee,<sup>1,†</sup> N. J. Upadhyay,<sup>1,‡</sup> and B. K. Jain<sup>1,§</sup>

<sup>1</sup>*Department of Physics, University of Mumbai,*

*Vidyanagari, Mumbai - 400 098, India.*

(Dated: December 1, 2018)

## Abstract

$p\Lambda$  emission in coincidence following  $K^-$  absorption at rest in nuclei is studied using quantum mechanical scattering theory and nuclear wave functions.  $K^-$  absorption is assumed to occur on two protons in the nucleus. In the formalism, emphasis is put on the study of the final state interaction (FSI) effects of  $p$  and  $\Lambda$  with the recoiling nucleus. We include elastic scattering and single nucleon knock-out (KO) channels in the FSI. Calculations are presented for the  $^{12}\text{C}$  nucleus, using shell model wave functions, and without any extra mass modification of the  $K^-pp$  system in the nucleus. Calculated results are presented for the angular correlation distribution between  $p$  and  $\Lambda$ , their invariant mass distribution and the momentum spectra of  $p$  and  $\Lambda$ . These results are compared with the corresponding experimental measurements [1]. With only elastic scattering FSI included, the angular correlation distribution and the momentum spectra are found to be in good accord with the corresponding measurements. With full FSI the calculated  $p\Lambda$  invariant mass distribution is found to have two peaks, one corresponding to the elastic scattering FSI and another to single nucleon KO FSI. The KO peak agrees fully, in position and shape, with the peak observed in Ref. [1]. The peak corresponding to elastic scattering FSI does not seem to exist in the measured distribution. Considering that such a two peak structure is always seen in the inclusive  $(p, p')$  and  $(e, e')$  reactions in nuclei at intermediate energies, absence of the elastic scattering peak in the  $p\Lambda$  reaction is intriguing.

PACS numbers: 25.80.Nv, 25.80.Dj, 13.75.Jz, 21.45.-v

---

\* to appear in Phys. Rev. C

<sup>†</sup>Electronic address: grishmamehta1982@yahoo.com

<sup>‡</sup>Electronic address: njupadhyay@gmail.com

<sup>§</sup>Electronic address: brajeshk@gmail.com; Present Address: UM-DAE, Centre for Excellence in Basic Sciences, University of Mumbai, Vidyanagari, Mumbai - 400 098, India.



## I. INTRODUCTION

The  $K^-p$  interaction is attractive in s-wave and isospin,  $T = 0$  state. Because of this there is much interest in its study and the study of its implications in the possible existence of the  $K^-$ -nucleus quasi-bound states in nuclei. Experimentally, the existence of such bound states is indicated in the FINUDA measurements [1] of the stopped  $K^-$  absorption on Li, C and other target nuclei. These experiments using the FINUDA spectrometer installed at the DAΦNE collider detect a  $\Lambda$  hyperon and a proton pair in coincidence following  $K^-$  absorption at rest on several nuclei. The emitted  $\Lambda$ - $p$  pair is found to emerge, predominantly back to back in all target nuclei, and have their invariant mass distributions peaking significantly below the sum of a kaon and two proton mass in free state (2.370 GeV). If it is assumed that the  $\Lambda$ - $p$  pair is emitted from a “ $K^-pp$ ” system in the nucleus, this mass shift implies a bound  $K^-pp$  system in nuclei with the binding energy above 100 MeV. In a more elaborate second run of these experiments carried out recently [2] it is further reported that these mass shifts occur only for the  $K^-pp$  module, and not for the  $K^-np$  cluster. The absorption on an  $np$  pair gives  $\Lambda$ - $n$  and  $\Sigma^-$ - $p$  pairs in the final state.

Recent analysis of the old DISTO data from the Saturne accelerator on  $pp \rightarrow p\Lambda K^+$  reaction too suggests the existence of a  $K^-pp$  cluster with the binding energy around 100 MeV [3].

Theoretically, following the extraordinary success of the SU(3) chiral perturbation theories in describing the  $\pi$ - $N$  and  $K^+$ - $N$  systems, the  $K^-$ - $p$  system has also been studied under this framework, though, unlike pion and  $K^+$  cases, the basic interaction here is relatively strong. This, however, is incorporated in these studies by including terms up to order  $q^2$  in the chiral Lagrangian expansion. Then, in combination with non-perturbative coupled-channel techniques this framework has been found quite appropriate for the study of antikaon-nucleon interaction in the literature. It was first developed in Ref. [4], and subsequently expanded in Ref. [5]. Various channels involved for  $S = -1$  meson-baryon scattering are  $\pi^+ \Sigma^-$ ,  $\pi^0 \Sigma^0$ ,  $\pi^- \Sigma^+$ ,  $\pi^0 \Lambda$ ,  $K^- p$ ,  $K^0 n$ . With the proper choice of parameters entering in these calculations, all available low-energy scattering data in these channels are reproduced well. The  $K^-p$  scattering amplitude resulting from these calculations have a two pole structure between  $\Sigma\pi$  and  $\bar{K}N$  thresholds. The pole which is located close to the real axis couples strongly to the  $\bar{K}N$  channel, while the one coupling strongly to  $\pi\Sigma$



channel lies away from the real axis. Empirically, only available information pertaining to  $K^- p$  scattering below threshold is the  $\Sigma \pi$  invariant mass distribution. This mass spectrum has its maximum at 1405 MeV, and has a width of about 50 MeV. In the Particle Data Group table [6] this is identified as  $T = 0$ , spin half,  $S = -1$   $\Lambda(1405)$   $K^- p$  bound state with a binding energy of 27 MeV. However, it is noticed in the literature that there is some subtlety involved in assigning a mass to the  $\Lambda(1405)$ . The observed  $\Sigma \pi$  spectrum has  $T = 0$ . Hence, in principle, it can have a generic s-wave  $T = 0$  source. This means that one needs to fit a superposition of the contributions from both, the  $\bar{K} N$  and  $\Sigma \pi$  poles mentioned above, to reproduce the observed  $\Sigma \pi$  spectrum and assign a mass to  $\Lambda(1405)$ . Within this scenario it turns out that both the poles contribute roughly in equal measure to reproduce the measured  $\Sigma \pi$  spectrum, with a tendency towards higher  $\bar{K} N$  share. A more thorough investigation of this issue has been carried out recently in Ref. [7]. They conclude that for the study of  $\bar{K} N$  scattering, amongst various channels involved in the coupled channel calculations, the  $\bar{K} N$  and  $\Sigma \pi$  channels dominate and they couple strongly. They also conclude that the mass of the  $\Lambda(1405)$  state is in fact 1420 MeV, and not 1405 MeV, thus making it only 12 MeV below  $\bar{K} N$  threshold.

Recent measurements on the  $pp \rightarrow p K^+ Y^0$  reaction at COSY [8], however, seem to present experimental evidence which do not support the above two pole model for the  $\Lambda(1405)$ . The shape and position of the  $\Lambda(1405)$  distribution in these measurements is reconstructed cleanly in the  $\Sigma^0 \pi^0$  channel using invariant- and missing-mass techniques. The mass of the  $\Lambda(1405)$  is found to be  $\sim 1400$  MeV and width  $\sim 60$  MeV.

Theoretical search for the antikaon-nucleus bound state has been carried out in the literature following the variational approach [9, 10] and the Faddeev method [11] for  $K^-$  plus 2-3 nucleons and heavier nuclei. All these calculations need, as input, realistic choice for the  $NN$  and the  $K^-N$  potentials. For the nucleon-nucleon potential, following extensive work over the years on this subject, it is always possible to make a correct choice. For the  $K^-N$  potential, however, the situation is uncertain. Some calculations generated a pseudo-potential for it by reproducing the  $K^-p$  bound state of 27 MeV binding energy, while others used a leading order chiral interaction. They all found  $K^- pp$  bound states with about 50 MeV or more binding energies. Latest calculation in Ref. [10], which, following the two pole model, uses the  $K^-N$  effective potential corresponding to 1420 MeV mass of  $\Lambda(1405)$ , finds a  $K^- pp$  system bound by around 19 MeV only. This state has a width between 40 and 70



MeV. This suggests that the  $K^- pp$  module might not be sufficiently bound to produce any experimentally observable signal corresponding to the antikaon-nucleus mesic bound state.

The situation is further confused by the suggestion in Ref. [12], that the down-shift observed in the invariant mass of the  $p$  and  $\Lambda$  in the FINUDA experiment could be the result of the final state interaction of these particles with the recoiling nucleus. This seems quite plausible because, due to Q-value of the  $K^- + pp \rightarrow \Lambda p$  reaction being around 317 MeV, the kinetic energies of outgoing  $p$  and  $\Lambda$  are 160 MeV or so. At these energies, it is well known that in the nucleon-nucleus scattering the reactive cross section mainly consists of the single nucleon knock-out channel [13]. Thus, the knock-out of one nucleon in the nucleus by the out going  $p$  or  $\Lambda$  can shift their energies considerably. The calculations in Ref. [12] indeed reproduce the observed mass shifts in the FINUDA experiments. However, as mentioned earlier, the similar effects not observed in Run (2) of FINUDA in  $K^-pn$  absorption can not be reconciled with this explanation [2].

Therefore, the situation on the  $(K^-, p\Lambda)$  reaction in the nucleus seems very confusing. It calls for more studies on the description of the reaction dynamics, as well as the  $K^-$ -nuclear binding.

In the present paper we reexamine the hypothesis of Magas *et al.* [12] of the origin of the observed  $\Lambda$ - $p$  peak in the FINUDA measurements to the single nucleon knock-out events in the final state. The calculations reported in Ref. [12] are the computer simulations of the internuclear cascade model for the nucleon-nucleus scattering. This approach describes the sequence of nucleon-nucleon collisions of the outgoing nucleon while passing through the residual nucleus in the final state in the framework of classical physics. The trajectory of each nucleon is followed. After a mean free path a  $N$ - $N$  collision takes place and its results are computed by Monte Carlo or some similar method. Apart from the Pauli principle there are no quantum mechanical effects in this approach of describing the FSI. The nucleus too is described by the Fermi gas model, thus being totally devoid of any nuclear structure effect. In view of the crucial role played by the FSI in interpreting the FINUDA  $\Lambda$ - $p$  measurements for  $K^-$ -nuclear bound states, it is absolutely necessary that the FSI in this reaction is described using quantum mechanical scattering theory and nuclear wave functions. This is the purpose of the present paper.

The paper is organized as follows. In Section 2, first, based on physical reasoning, we present an overall description of the  $(K^-, \Lambda p)$  reaction following  $K^-$  absorption in the



nucleus along with an appropriate final state interaction. This is followed by the formalism utilized for the evaluation of the cross section. Calculated results along with a discussion around them are presented for  $^{12}\text{C}$  target nucleus. This is followed by the conclusions.

To remain specific in our discussion and presentation, in the following we consider  $^{12}\text{C}$  target nucleus all along.

## II. GENERAL DISCUSSION

### A. $K^-$ absorption

The  $K^-$  meson after being captured in a high atomic orbit reaches the  $3d$  orbit through electromagnetic transitions. From there onward it comes under the influence of the strong nuclear interaction and gets absorbed. The X-ray transition width for the  $3d \rightarrow 2p$  transition and the nuclear capture from the  $3d$  orbit are reported in [26] to be 0.0749 eV and  $0.98 \pm 0.19$  eV respectively. This gives the relative population of kaons in  $2p$  and  $3d$  orbits, using

$$\frac{P(2p)}{P(3d)} = \frac{\Gamma_X(3d \rightarrow 2p)}{\Gamma_X(3d \rightarrow 2p) + \Gamma_a(3d)} \quad (1)$$

around 7%. Such a small population of kaons in the  $2p$  orbit also makes nuclear capture of kaons from the  $1s$  orbit as insignificant. We, thus, consider in our calculations the capture of the kaon from both the  $3d$  and  $2p$  atomic orbits. The  $K^-$  absorption yield for the  $p\Lambda$  branch is written as the weighted average yield from these orbits as

$$\omega(p\Lambda) = \omega_{3d}(p\Lambda) + 0.07 \omega_{2p}(p\Lambda). \quad (2)$$

However, as we will see later (Fig. 1), due to larger centrifugal barrier, the overlap of the  $3d$  orbit with the nuclear wave functions is about 2 orders of magnitude smaller than that of the  $2p$  orbit. Furthermore, as the calculation of the absorption yield,  $\omega$  involves the square of this overlap, despite the factor of 0.07 in the above for the  $2p$  orbit, the contribution from the  $3d$  orbit to the  $K^-$  nuclear capture remains about two orders of magnitude smaller than that from the  $2p$  orbit. Therefore, in the following we present calculations considering the capture from the  $2p$  orbit only.

In the absorption process, the  $\Lambda$  hyperons in the final state are produced either in the quasi-free process  $K^- N \rightarrow \Lambda \pi$  or the two-nucleon absorption process  $K^- N N \rightarrow \Lambda N$ .



For the measurements which involve  $p$ - $\Lambda$  detection in coincidence, obviously only the two-nucleon absorption contributes. The absorption on more than two nucleons is expected to be weak because the probability of finding three or more nucleons together in the nucleus is small. The  $Q$ -value of the  $K^- NN \rightarrow \Lambda N$  process (ignoring nuclear binding of the absorbing protons) is 317 MeV. This energy is mainly shared by the emerging nucleon and the  $\Lambda$  hyperon. Furthermore, since the Fermi momentum of the nucleons in the nucleus is not large, the outgoing nucleon and the  $\Lambda$  hyperon following  $K^-$ -absorption at rest emerge back to back and have their momenta centred around 570 MeV/c. Of course, due to Fermi motion, in an actual situation the back to back correlation is smeared into two narrow cones, and momenta of the nucleon and the  $\Lambda$  are spread around 570 MeV/c by the Fermi motion. Additionally, the target nucleus, after absorption, is left into a two hole shell model state.

Structurally, two aspects of nucleon motion in the nucleus appear in the  $(K^-, p\Lambda)$  absorption process in the nucleus. Because of the predominantly back to back emission of  $p$  and  $\Lambda$  hyperon and their momenta being centred around 570 MeV/c, the absorbing pair of nucleons in the nucleus needs to be as close as around 0.2 fm to each other at the time of  $K^-$  absorption. Since the  $N$ - $N$  potential at these distances is very strong, the relative wave function of these protons has strong short range correlations. These correlations in the nucleus, however, heals very fast [14] and the wave function goes over to the shell model mean field wave function. The centre of mass of these two protons, however, has no such constraints on it, hence, it always moves in the most probable trajectory given by the nuclear mean field. The appropriate 2-proton wave function in the nucleus for the kaon absorption, therefore, has the form,

$$\Psi_{pp}(\vec{r}_1, \vec{r}_2) = \psi_p(\vec{r}_1) \psi_p(\vec{r}_2) f(r), \quad (3)$$

where  $\psi$ 's are the shell model wave functions and  $f(r)$  is a Jastrow-type correlation function [15].

The outgoing  $p$  and  $\Lambda$  will also be correlated similarly by a correlation function, say  $f'(r)$ . The healed  $p$ - $\Lambda$  wave function here, however, will be a phase shifted wave function.

Consequent to the above completely two different space scales involved, the absorption probability for  $K^-$  in the nucleus for the  $p$ - $\Lambda$  branch (for absorption on a  $pp$  pair, say) factors into two parts (shown in the next section),

$$\omega_{abs}(\vec{p}_p, \vec{p}_\Lambda) = g_{abs}(q) G(Q), \quad (4)$$



where  $\vec{q} = (m_p \vec{p}_\Lambda - m_\Lambda \vec{p}_p)/(m_p + m_\Lambda)$  and  $\vec{Q} = \vec{p}_p + \vec{p}_\Lambda$  are the centre-of-mass and the total momenta of the  $p$  and  $\Lambda$  respectively.  $g$  and  $G$  are respectively the absorption strength for  $K^- pp \rightarrow p\Lambda$  process in their centre of mass and the momentum probability distribution of nuclear wave functions corresponding to the total momentum,  $Q$ . Because of the back-to-back emission of  $p$  and  $\Lambda$ , obviously the magnitude of  $q$  is very large and that of  $Q$  is small. Due to these vastly different momentum scales for  $q$  and  $Q$ , over most of the variables measured in the  $(K^-, p\Lambda)$  reaction, while  $G(Q)$  can go through a large variation, the factor  $g(q)$  does not change much.

### B. Final State Interaction

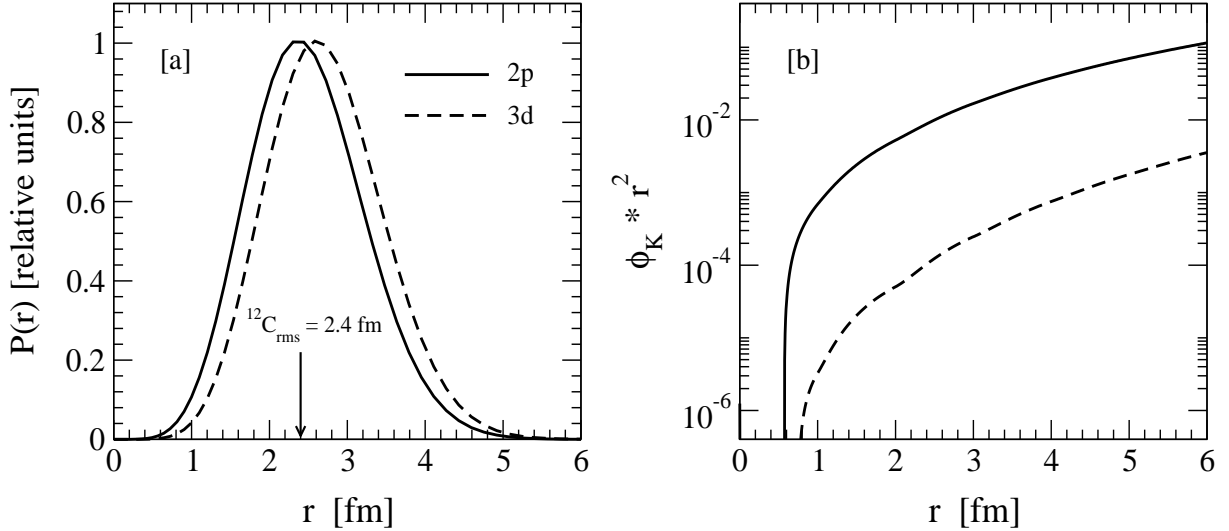


FIG. 1: (a) Overlap function,  $P(r)$  showing the localization of the  $K^-$  absorption for the 2p and 3d orbits. The vertical line shows the *rms* radius of the  $^{12}\text{C}$  nucleus. (b) Distribution of the 2p and the 3d  $K^-$  wave functions.

Before we talk about the final state interaction (FSI), let us mention that the  $K^-$  absorption in the nucleus occurs on its surface. Quantitatively, this region is determined by the overlap of the  $K^-$  2p and 3d atomic orbits with the spatial distribution of the absorbing protons. Fig. 1a shows these overlaps, where

$$P(r) = r^2 \phi_K(r) \psi_{p_1}(r) \psi_{p_2}(r). \quad (5)$$



For the  $^{12}\text{C}$  nucleus we have taken the two protons moving in the  $1p$  shell model orbital. Their radial distribution is described by the harmonic oscillator wave function. The kaonic atomic orbits are given by the hydrogenic wave function. To show their relative localization clearly, in Fig. 1a we plot  $P(r)$ 's for the  $2p$  and the  $3d$   $K^-$  orbits, which have different magnitudes, on the same scale with arbitrary units. We see that both the overlap functions peak around  $r = 2.5$  fm, with  $3d$  overlap function about half a fermi ahead. The  $^{12}\text{C}$  rms radius is known to be 2.4 fm. The magnitude of the  $3d$  overlap function, we note is two orders of magnitude smaller than that of the  $2p$  orbit. This happens because the  $3d$  wave function rises slower than the  $2p$   $K^-$  wave function in the region of the overlap, as we see in Fig. 1b.

Above localization of the  $P(r)$  beyond the  $^{12}\text{C}$  rms radius coupled with the back to back emission of  $p$  and  $\Lambda$  following absorption, suggests that only one of the two emitted particles,  $p$  and  $\Lambda$ , goes into the nucleus at a time. The other particle moves outward. Hence, the FSI with the recoiling nucleus is mainly suffered by only one particle,  $p$  or  $\Lambda$  at a time. The channels which dominate in contribution to this interaction are the elastic channel and the single nucleon knock-out (KO) channel. The latter is known to constitute about 80% of the total reactive cross section in the proton-nucleus inelastic scattering in nuclei around 160 MeV proton energy [13], which is the relevant proton energy in the present study. Out of these, the effect of the elastic channel at intermediate energies is mostly absorptive, while that of the KO channel is dispersive as well as absorptive. In our calculations, we include both the channels. The inclusive probability for a process like

$$K^- + A \rightarrow p + \Lambda + X, \quad (6)$$

is therefore written as

$$d\omega = d\omega_{elas} + d\omega_{KO}. \quad (7)$$

The sum of two terms in the above is incoherent because in principle (by making exclusive measurements) we can distinguish between elastic scattering and single scattering with one target nucleon being knocked out.



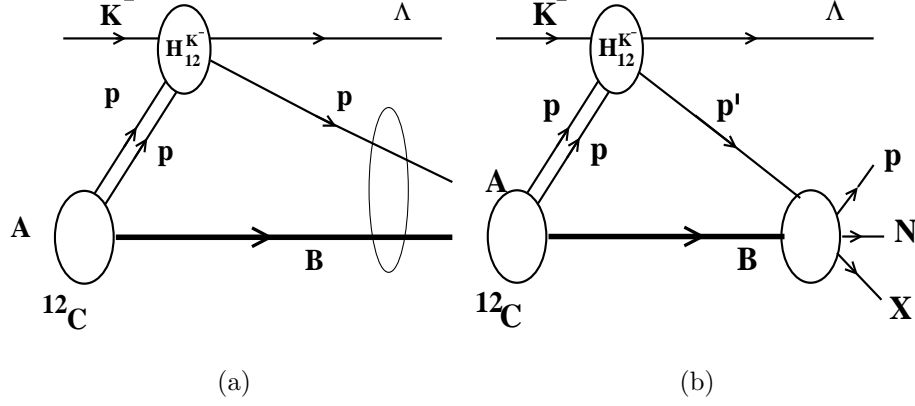


FIG. 2: Reaction mechanism of (a) Elastic process and (b) Knock-out process.

### III. FORMALISM AND RESULTS

#### A. Elastic

The “elastic” process for the  $A(K^-, p\Lambda)B$  reaction is shown in Fig. 2a. In it the  $K^-$  gets absorbed on a pair of protons in the target nucleus and produces a  $p\Lambda$  pair. This pair is detected in coincidence in the final state. No measurements are made on the recoiling nucleus, hence the measurements are inclusive in that sense. The recoiling nucleus is left in a *two hole* state centred around the excitation corresponding to the summed binding energy ( $B_1 + B_2$ ) of nucleons 1 and 2 in the nucleus A. Let us denote different states of B around this excitation by  $n$ . The inclusive absorption probability for protons in shells ( $n_1 l_1; n_2 l_2$ ) in the nucleus is then given by

$$d\omega_{elas} = \frac{1}{(2\pi)^5} \sum_n \delta(M_i - T_\Lambda - T_p - T_B - E_n^*) \delta(\vec{P}_B + \vec{p}_p + \vec{p}_\Lambda) \times d\vec{p}_p d\vec{p}_\Lambda d\vec{P}_B \sum_{\sigma} |M_{fi}|^2, \quad (8)$$

where  $M_i = m_K + m_p - m_\Lambda$  and  $E_n^*$  is the excitation energy of the state  $n$  in  $B$ .  $T_x$  denotes the kinetic energy of the particle  $x$ . Bar on the sum in the above expression denotes the average and sum over the spins in the initial and final states respectively. The transition matrix element  $M_{fi}$  is given by

$$M_{fi} = [N_{l_1 l_2}]^{1/2} \int d\xi dx_1 dx_2 \Psi_{B,n}^*(\xi) \chi^{-*}(x_1, x_2) H_{12}^{K^-} \Psi_A(\xi, x_1, x_2) \phi_K, \quad (9)$$



where  $N_{l_1 l_2}$  are the active number of absorbing proton pairs in shell  $(n_1 l_1; n_2 l_2)$  in the target nucleus,  $A$ .  $\Psi_x$  is the nuclear wave function, and  $\chi$  is the elastically scattered  $p$  and  $\Lambda$  wave function.  $H_{12}^{K-}$  is the absorption vertex, and it depends only on the proton coordinates,  $x_1$  and  $x_2$  in the nucleus  $A$ .  $\xi$  represents collectively the coordinates of the  $(A - 2)$  nucleons.

To proceed further we note that since the excited states ‘ $n$ ’ in the nucleus  $B$  are the hole states corresponding to two nucleons, they are not likely to have much energy spread. Hence, in the energy delta function in Eq. (8) we replace  $E_n^*$  by  $|B_1 + B_2| = B_{12}$ . With this we obtain

$$d\omega_{elas} = [PS] \sum_n \sum_{\sigma}^{\bar{}} |M_{fi}|^2, \quad (10)$$

with  $[PS]$ , the phase space factor, given by

$$[PS] = \frac{1}{(2\pi)^5} \delta(M_i - T_{\Lambda} - T_p - T_B - B_{12}) d\vec{p}_{\Lambda} d\vec{p}_p, \quad (11)$$

and  $\vec{P}_B = -(\vec{p}_p + \vec{p}_{\Lambda}) = -\vec{Q}$ . Sum over ‘ $n$ ’ is now performed using the “closure relation”, yielding

$$\begin{aligned} \sum_{\sigma} \sum_n^{\bar{}} |M_{fi}|^2 &\equiv |\bar{M}_{fi}|^2 \\ &= [N_{l_1 l_2}] \sum_{\sigma}^{\bar{}} \int d\xi \left| \int dx_1 dx_2 \chi^{-*}(x_1, x_2) H_{12}^{K-} \Psi_A(\xi, x_1, x_2) \phi_K \right|^2. \end{aligned} \quad (12)$$

Since we are interested only in the inclusive absorption strength we take a simple description of the target nucleus, where the absorbing protons move in shell model orbitals  $(n_1 l_1)$  and  $(n_2 l_2)$  and the core of  $(A-2)$  nucleons is a spectator. With this description, above expression reduces to

$$|\bar{M}_{fi}|^2 = [N_{l_1 l_2}] \sum_{\sigma}^{\bar{}} \left| \int dx_1 dx_2 \chi^{-*}(x_1, x_2) H_{12}^{K-} \Psi_{n_1 l_1 m_1; n_2 l_2 m_2}(x_1, x_2) \phi_K \right|^2, \quad (13)$$

where  $\Psi_{n_1 l_1 m_1; n_2 l_2 m_2}(x_1, x_2)$  is the properly anti-symmetrized two proton wave function in the nucleus. In the  $LS$  representation it is written as

$$\begin{aligned} \Psi_{n_1 l_1 m_1; n_2 l_2 m_2}(x_1, x_2) &= \sum_{LMS\sigma} (l_1 l_2 m_1 m_2 / L M) (1/2 \ 1/2 \ \sigma_1 \ \sigma_2 / S \sigma) \\ &\quad \times \phi_{LM}(\vec{r}_1, \vec{r}_2) \chi_{S\sigma}(\vec{s}_1, \vec{s}_2). \end{aligned} \quad (14)$$

For two protons in the same shell antisymmetry requires that  $L + S = \text{even}$ . Further on, performing sum over  $m_1, m_2, \sigma_1$  and  $\sigma_2$  contained in  $\sum_{\sigma}^{\bar{}}$  in Eq. (13), we get



$$|\bar{M}_{fi}|^2 = N_{l_1 l_2} \frac{1}{4} \sum_{S\sigma} \frac{1}{(2l_1 + 1)(2l_2 + 1)} \times \sum_{LM} \left| \int dx_1 dx_2 \chi^{-*}(x_1, x_2) H_{12}^{K-} \phi_K \phi_{LM}(\vec{r}_1, \vec{r}_2) \chi_{S\sigma}(\vec{s}_1, \vec{s}_2) \right|^2. \quad (15)$$

The correlation functions  $f(r)$  and  $f'(r)$  mentioned in Eq. (3) and after it are absorbed here in the absorption vertex  $H_{12}^{K-}$ .

### 1. Evaluation of $|\bar{M}_{fi}|^2$

To proceed further, let us now utilize the fact that the momentum  $\vec{q}$  appearing in the absorption vertex  $H_{12}^{K-}$  has large magnitude and a short range. Because of this, in the expression for  $|\bar{M}_{fi}|^2$  we can factorize the expectation value of  $H_{12}^{K-}$  from the rest, and write,

$$|\bar{M}_{fi}|^2 = \left[ \frac{1}{4} \sum_{S\sigma} \left| \langle p, \Lambda, \vec{q} | H_{12}^{K-} | \chi_{S\sigma}(\vec{s}_1, \vec{s}_2), ppK^- \rangle \right|^2 \right] \times \left[ \frac{N_{l_1 l_2}}{(2l_1 + 1)(2l_2 + 1)} \sum_{LM} \left| \int d\vec{r}_1 d\vec{r}_2 \chi^{-*}(\vec{r}_1, \vec{r}_2) \phi_K(\vec{r}_1) \phi_{LM}(\vec{r}_1, \vec{r}_2) \delta(\vec{r}_1 - \vec{r}_2) \right|^2 \right]. \quad (16)$$

Two expressions in the square brackets in above can be identified with two terms of Eq. (4), i.e.

$$g_{abs}(q) = \left[ \frac{1}{4} \sum_{S\sigma, \sigma_p, \sigma_\Lambda} \left| \langle p, \Lambda, \vec{q} | H_{12}^{K-} | \chi_{S\sigma}(\vec{s}_1, \vec{s}_2), ppK^- \rangle \right|^2 \right], \quad (17)$$

and

$$G(Q) = [PS] N_{l_1 l_2} \frac{1}{(2l_1 + 1)(2l_2 + 1)} \times \sum_{LM} \left| \int d\vec{r}_1 d\vec{r}_2 \chi^{-*}(\vec{r}_1, \vec{r}_2) \phi_K(\vec{r}_1) \phi_{LM}(\vec{r}_1, \vec{r}_2) \delta(\vec{r}_1 - \vec{r}_2) \right|^2. \quad (18)$$

### 2. Distorted waves $\chi's$

As the energies of the proton and the lambda following  $K^-$  absorption is around 160 MeV or so, we describe the scattering of these particles by the recoiling nucleus using eikonal approximation. The basic assumption in this description is that the propagating particle is



mainly scattered in the forward direction. Taking z-axis parallel to the proton momentum,  $\vec{p}_p$ , the proton distorted wave,  $\chi_{\vec{p}_p}^{-*}$  is written in eikonal approximation as

$$\chi_{\vec{p}_p}^{-*}(\vec{r}) = e^{-i\vec{p}_p \cdot \vec{r}} D_{\vec{p}_p}(\vec{r}), \quad (19)$$

where the distortion function  $D$  is given in terms of an optical potential,  $V_p$  by

$$D_{\vec{p}_p}(\vec{r}) \equiv D_{\vec{p}_p}(\vec{b}, z) = \exp \left[ -\frac{i}{\hbar v_p} \int_z^\infty V_p(\vec{b}, z') dz' \right], \quad (20)$$

where  $\vec{r} = (\vec{b}, z)$ . For writing the  $\Lambda$  distorted wave we recall that the  $\Lambda$  moves opposite to the proton. Therefore, the momentum vector  $\vec{p}_\Lambda$  is anti-parallel to the chosen z-axis. The distortion factor,  $D_{\vec{p}_\Lambda}(\vec{r})$  for  $\Lambda$  therefore becomes [16]

$$D_{\vec{p}_\Lambda}(\vec{r}) = \exp \left[ -\frac{i}{\hbar v_\Lambda} \int_{-\infty}^z V_\Lambda(\vec{b}, z') dz' \right]. \quad (21)$$

Combining  $D$ 's for the proton and the lambda we then get

$$D_{\vec{p}_p}(\vec{r}) D_{\vec{p}_\Lambda}(\vec{r}) = \exp \left[ -\frac{i}{\hbar} \left( \int_{-\infty}^z \frac{V_\Lambda}{v_\Lambda} dz' + \int_z^\infty \frac{V_p}{v_p} dz' \right) \right]. \quad (22)$$

If we make the “ $t\rho$ ” approximation for  $V$ 's and assume forward scattering for  $t$ , we get

$$D_{\vec{p}_p}(\vec{r}) D_{\vec{p}_\Lambda}(\vec{r}) = \exp \left[ \frac{i}{2} \left( \sigma_T^{\Lambda N} (i + \beta_{\Lambda N}) \int_{-\infty}^z \rho dz' + \sigma_T^{pN} (i + \beta_{pN}) \int_z^\infty \rho dz' \right) \right], \quad (23)$$

where  $\sigma_T^x$  and  $\beta_x$  are respectively the total cross section and the ratio of the real to imaginary part of the scattering amplitude for the  $xN$  system.

Now, if we ignore the difference between the proton and the lambda elementary scattering parameters and take them as that for the better studied  $pN$  system at some mean value of the  $p$  and  $\Lambda$  energies, above expression simplifies to

$$\begin{aligned} D_{\vec{p}_p}(\vec{r}) D_{\vec{p}_\Lambda}(\vec{r}) &\equiv D(\vec{r}) = \exp \left[ \frac{i}{2} \sigma_T^{pN} (i + \beta_{pN}) \int_{-\infty}^\infty \rho(\vec{r}') dz' \right] \\ &= \exp \left[ \frac{i}{2} \sigma_T^{pN} (i + \beta_{pN}) T(\vec{b}) \right], \end{aligned} \quad (24)$$

where  $\rho(r)$  is the nuclear density and  $T(\vec{b})$  is the total nuclear material seen by the proton and the lambda *together* at an impact parameter,  $\vec{b}$ . It is given by

$$T(\vec{b}) = \int_{-\infty}^\infty \rho(\vec{r}') dz', \quad (25)$$



with  $r' = \sqrt{b^2 + z'^2}$ . Now if we observe Eq. (24) for  $D(\vec{r})$  a little closely, we realize that this, in fact, is the total distortion factor for the passage of a proton from one end of the nucleus to another. This, thus, is the mathematical description for the statement made in an earlier Section that, because of the peripheral localization of the  $K^-$  absorption and the back-to-back emission of  $p$  and  $\Lambda$ , total scattering of the  $p$  and the  $\Lambda$  can be included in the final state by considering the passage of only one particle ( $p$  or  $\Lambda$ ) through the whole nucleus.

Furthermore, since the effect of distortion at the energies of  $p$  and  $\Lambda$  in the studies here ( $\sim 160$  MeV) is mainly absorptive, and most of the measurements on  $p\Lambda$  following  $K^-$ -absorption are of inclusive type, it will be reasonably correct to include the overall effect of the distortion in  $G(Q)$  by multiplying it by an attenuation factor,  $\eta_A(T_p)$ , given by

$$\begin{aligned}\eta_A(T_p) &= \frac{\int d\vec{b} dz \rho_A(\vec{b}, z) |D(\vec{r})|}{\int d\vec{b} dz \rho_A(\vec{b}, z)} \\ &= \frac{\int d\vec{b} dz \rho_A(\vec{b}, z) e^{-\frac{1}{2}(P\sigma_T^{pN}(T_p)) T(\vec{b})}}{\int d\vec{b} dz \rho_A(\vec{b}, z)},\end{aligned}\quad (26)$$

and removing the distortion factor from the integral in Eq. (18). Factor  $P$  in above has been introduced before  $\sigma_T^{pN}$  to include the effect of Pauli-blocking of the nucleons in the nucleus after scattering. A nuclear matter estimate for its value above twice the Fermi energy is given by [17]

$$P(\epsilon) = 1 - \frac{7}{5\epsilon}, \quad (27)$$

where  $\epsilon = \frac{T_p}{E_F}$ , with  $E_F$  denoting the Fermi energy.

With above treatment of distortion, Eq. (18) for  $G(Q)$  simplifies to

$$G(Q) = [PS] |\eta_A(T_p)|^2 \sum_{LM} |F_{LM}^{l_1 l_2}(Q)|^2, \quad (28)$$

where

$$\begin{aligned}\sum_{LM} |F_{LM}^{l_1 l_2}(Q)|^2 &= \sum_{LM} \left| \sqrt{\frac{N_{l_1 l_2}}{(2l_1 + 1)(2l_2 + 1)}} \int d\vec{r}_1 e^{-i\vec{Q} \cdot \vec{r}_1} \phi_K(\vec{r}_1) \phi_{LM}(\vec{r}_1, \vec{r}_1) \right|^2 \\ &= N_{l_1 l_2} \sum_L (l_1 l_2 00 / L 0)^2 |g_{l_1 l_2}^L(Q)|^2,\end{aligned}\quad (29)$$

with

$$g_{l_1 l_2}^L(Q) = \int dr r^2 j_L(Qr) R_{n_1 l_1}(r) R_{n_2 l_2}(r) \phi_K(r), \quad (30)$$



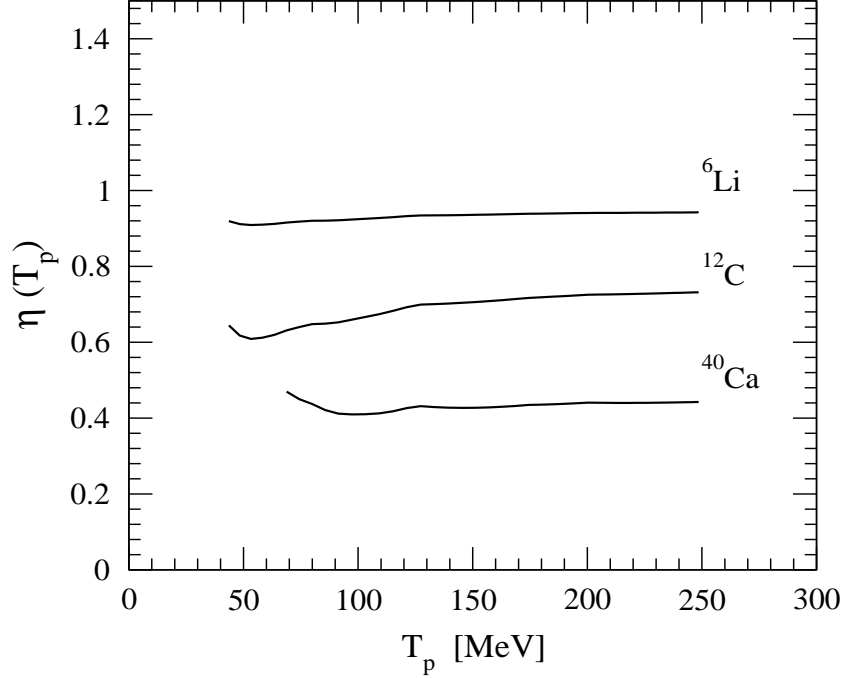


FIG. 3: Attenuation factor  $\eta_A(T_p)$  (Eq. (26)) for  ${}^6\text{Li}$ ,  ${}^{12}\text{C}$  and  ${}^{40}\text{Ca}$  nuclei.

where  $R_x$  are the nucleon radial wave functions in the nucleus.

The value of  $\eta_A(T_p)$  depends upon the proton energy,  $T_p$  through  $P\sigma_T^{pN}$  and upon the nucleus through the thickness function,  $T(b)$ . To get an idea about the value and its variation, in Fig. 3 we plot  $\eta_A(T_p)$  in the proton kinetic energy range 50-250 MeV for three nuclei,  ${}^6\text{Li}$ ,  ${}^{12}\text{C}$  and  ${}^{40}\text{Ca}$ . For calculating the Pauli blocking factor,  $P$ , Fermi momentum is taken equal to 200 MeV/c. The nuclear densities are taken from Ref. [18]. We find that in the energy range (100-200 MeV) of interest in the present calculations the attenuation factor approximately remains constant. The values of this factor for the three nuclei are around 0.9, 0.7 and 0.4 respectively.

### 3. Absorption Vertex, $g_{abs}(q)$

Prescription to describe the absorption vertex,  $g_{abs}(q)$  is not clear and also not simple. One thing, which is definite about it is that, it involves large momentum transfer, hence, spatially it can not be localized over any extended volume. Dynamically, the one-nucleon absorption mechanism,  $K^-p \rightarrow \pi\Lambda$  is understood to involve the  $\Lambda(1405)$ , which decays in to



a pion and a hyperon. The range of this vertex is determined by the  $\Lambda(1405)$  propagator. A study in Ref. [28] suggests that the absorption probability depends upon this range, and in their estimate this range could be around 0.75 fm or so. The two nucleon mechanism, due to strong attractive  $K^-p$  interaction in the  $T = 0$  state, involves dynamically a strongly correlated system of  $K^-pp$ , where the  $K^-$  is continuously exchanged between two protons. Detailed dynamical composition of this system is determined in the  $\chi$ PTs by the non-perturbative coupling amongst various  $S = -1$ ,  $T = 0$  channels,  $\pi^+ \Sigma^-$ ,  $\pi^0 \Sigma^0$ ,  $\pi^- \Sigma^+$ ,  $\pi^0 \Lambda$ ,  $K^- p$ ,  $K^0 n$ . This system eventually decays in to  $p\Lambda$ . Exact mechanism of this decay is not immediately obvious. However, in line with the one-nucleon  $K^-$  absorption, one mechanism could be that at some stage in the  $K^-pp$  system a  $\Lambda(1405)$  is produced, which, as suggested in Ref. [10], interacts with another proton through an exchange of pions or a pair of  $\pi$ - $K$  and goes over to the  $p\Lambda$  final state. In Ref. [10], using the range parameter 0.2- 1.2 fm for the absorption vertex the authors estimate the decay width of 2-8 MeV for the  $K^-pp$  system, with the maximum width occurring for the range around 0.7 fm. Thus, it appears that, even if the details of the absorption vertex is not known very clearly, two things are clear: (i) the magnitude of the two proton  $K^-$  capture depends upon the spatial extension of the absorption vertex, and (ii) the probable range of the vertex is such that the variation of the capture probability with momentum,  $q$  could not be very rapid.

The  $(K^-, p\Lambda)$  reaction measurements have been done on the distributions of the  $\Lambda$  (and proton) momentum, invariant  $p\Lambda$  mass, and their angular correlations. In all these distributions, as we will discuss in the next Section, each point involves a folding of  $g(q)$  and  $G(Q)$ . However, the values of  $q$  for all the measurements are large (around 500 MeV/c) and do not have much spread (only up to 10%). Because of this, the factor  $g_{abs}(q)$  (Eq. (17)) in the formalism enters in determining the absolute magnitude of the  $(K^-, p\Lambda)$  process only. The shapes of different distributions are determined by the factor  $G(Q)$ . Furthermore, as the available data from the experiments exist only in arbitrary units, we have taken  $g_{abs}(q)$  as a constant factor, denoted by  $C$ , in our calculations.

#### 4. Results

Before we present the results let us make some points about the FINUDA experiment. The  $\Lambda$ 's are detected in this experiment by reconstructing the invariant mass of the  $\Lambda$  decay



products,  $p$  and  $\pi^-$ . However, the restriction on the low momentum threshold for  $\pi^-$  in the FINUDA spectrometer is such that it cuts out the  $\Lambda$  hyperons with a momentum lower than 300 MeV/c. Therefore, the  $\Lambda$  from the quasifree process ( $K^- N \rightarrow \Lambda \pi$ ) in this experiment is hardly observed. Above around 400 MeV/c, since the main contribution comes from two-nucleon absorptions ( $K^- \text{“} NN \text{”} \rightarrow \Lambda N, \Sigma^0 N$ ), the FINUDA measurements have major contribution from this capture process. Furthermore, the measurements are done with the  $p$  and  $\Lambda$  in coincidence, with the cosine of the angle between them restricted as  $-1 \leq \cos \theta_{p\Lambda} \leq -0.8$ . The latter constraint is put because the cross section beyond these limits is insignificant (see Fig. 4).

For calculations, putting all factors together from the above Section, the differential absorption strength,  $d\omega$  for  $K^-$ -absorption on two protons in shell model orbitals,  $(n_1 l_1; n_2 l_2)$  is finally written as

$$d\omega_{elas} = [PS] C |\eta_A(T_p)|^2 N_{l_1 l_2} \sum_L (l_1 l_2 0 0 / L 0)^2 |g_{l_1 l_2}^L(Q)|^2, \quad (31)$$

where all the terms are as defined in above Sections. We present here calculated results using this expression for the  $^{12}\text{C}$  target nucleus with an appropriate phase space factor,  $[PS]$ . The proton wave functions in  $^{12}\text{C}$  are generated in an oscillator potential, whose length parameter,  $b$  is taken equal to 1.67 fm. This parameter fits the elastic electron scattering data on the  $^{12}\text{C}$  nucleus [18]. The binding energies of protons in  $1p$  and  $1s$  shells are taken as given by the  $(p, 2p)$  and  $(e, e'p)$  reactions [19]. For  $^{12}\text{C}$  they are 15.96 and 34.0 MeV respectively. The  $K^-$  absorption is considered to occur on proton pairs in  $1p$ ,  $1s$  and  $1s1p$  shells. The value of  $N_{l_1 l_2}$  for these absorptions is taken equal to the number of possible proton pairs in these shells, as an upper limit. They are in the ratio of  $(1p)^2 : (1s1p) : (1s)^2 :: 6 : 8 : 1$ .

The phase space factor,  $PS$  for calculating the angular correlation between the  $p$  and  $\Lambda$  and their momentum distribution is written as

$$PS = \frac{4\pi m_p m_\Lambda}{(2\pi)^5} \frac{|\vec{p}_p|^2 |\vec{p}_\Lambda|^2}{(m_\Lambda + m_B) |\vec{p}_\Lambda| + |\vec{p}_p| m_\Lambda \cos(\theta_{\Lambda p})} d\cos(\theta_{\Lambda p}) d|\vec{p}_\Lambda|. \quad (32)$$

In Fig. 4 we present the calculated angular correlation between the  $\Lambda$  and the proton along with the FINUDA measurements. We find them to agree very well with each other.



The steep rise in the distribution towards  $\theta_{\Lambda p} = 180^\circ$  is the strong confirmation of the two-proton absorption mechanism. Both the results are given in relative units.

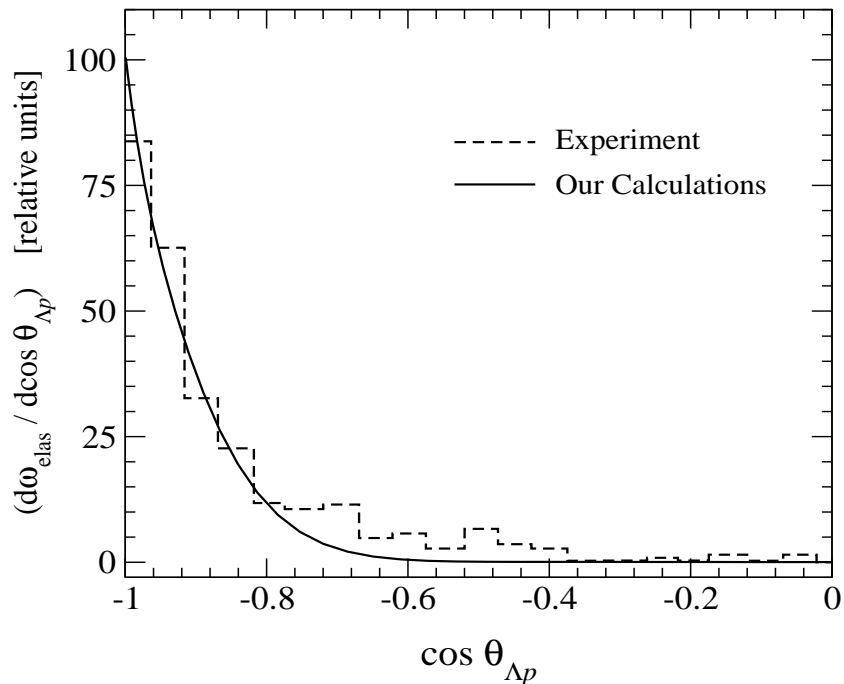


FIG. 4: Angular Correlation distribution between  $\Lambda$  and  $p$  along with the FINUDA measurements [1].

Measurements have also been done in the FINUDA experiment on the momentum distributions of the proton and  $\Lambda$ . The measured  $\Lambda$  distribution from Ref. [20] is shown in Fig. 5. If one believes that the observed  $p$  and  $\Lambda$  come from the two-proton absorption vertex and do not undergo any further FSI except the elastic scattering, this distribution should be similar to the one calculated using Eq. (31). We show the calculated  $\Lambda$  and proton momentum distributions in Fig. 5, and find that the peak position of the  $\Lambda$  distribution nearly agrees with the corresponding measured distribution. The shape of the calculated distributions is however found to be less broad compared to the observed one. Larger magnitude of measured events below 400 MeV/c, which makes it broader can not be understood easily. They can not be attributed to the quasifree process either because the FINUDA spectrometer cuts off  $\Lambda$ 's below 300 MeV/c. Another source of this deficiency can be that, in our calculations we have taken  $g_{abs}(q)$  (denoted by  $C$  in Eq. (31)) as constant. We examined it. As we see in the phase space expression (Eq. (32)), calculation of the absorption probability for each



value of the  $|\vec{p}_\Lambda|$  involves an integral over  $\cos(\theta_{p\Lambda})$ , which in the FINUDA measurements lies between  $-1.0$  and  $-0.8$ . This implies in the calculation for each  $p_\Lambda$  an integral over a certain range of  $q$  and  $Q$  corresponding to this range of  $p\Lambda$  angle. For 400, 500 and 600 MeV/c values of  $p_\Lambda$  (which more or less covers Fig. 5) this range of  $q$  is about 510-495, 520-505 and 515-500 MeV/c respectively. These values, as we see are large and have about same range for all the  $\Lambda$  momenta. Therefore our assumption about the constancy of  $g_{abs}(q)$  in the calculations should not be the cause of concern. The shape of the  $p_\Lambda$  distribution is, in fact, mainly determined by  $G(Q)$  through the  $Q$  dependence of the nuclear wave functions. The range of  $Q$  for the above three  $p_\Lambda$ 's in the  $-1 \leq \cos \theta_{p\Lambda} \leq -0.8$  are 200-260, 35-220, and 160-270 MeV/c respectively. This range shows why the  $p_\Lambda$  momentum distribution peaks around 500 MeV/c. It also suggests that it can probably be made broader by enriching the nucleon shell model wave functions in high momentum components. However, to reproduce the width of the observed momentum distribution, we believe that it will require a considerable modification of the nuclear wave function.

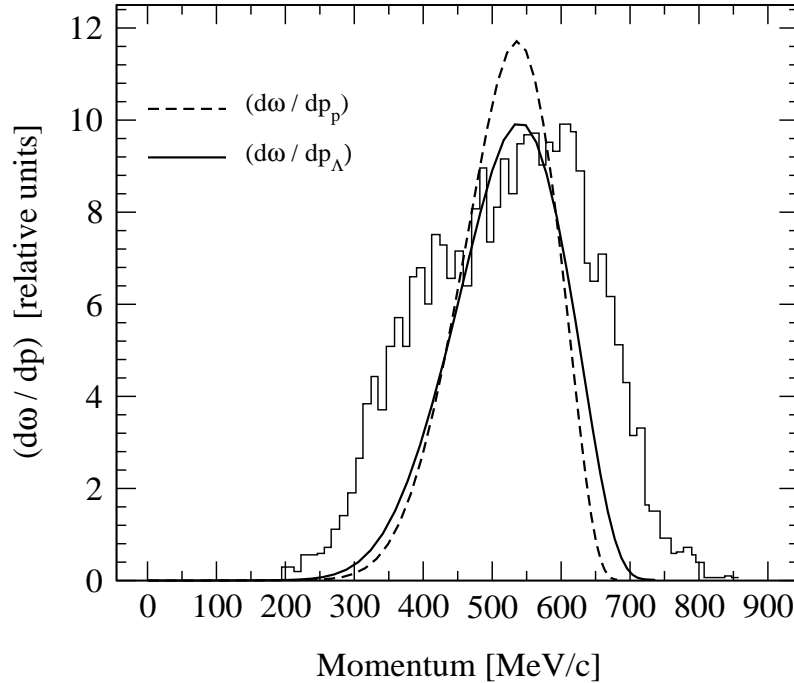


FIG. 5:  $\Lambda$  and  $p$  inclusive momentum distributions with  $-1 \leq \cos \theta_{p\Lambda} \leq -0.8$  along with the measured  $\Lambda$  momentum distribution (represented by Histogram).

Next we calculate the  $p$ - $\Lambda$  invariant mass distribution. The phase space for this is written



as

$$PS = \frac{4\pi \mu_{\Lambda p} \mu_{(\Lambda+p)B}}{(2\pi)^5} |\vec{Q}| |\vec{q}| dM_{\Lambda p} d\cos(\theta_{Qq}), \quad (33)$$

where  $\mu_{xy}$  denotes the reduced mass of the  $x, y$  system. The magnitudes of  $\vec{Q}$  and  $\vec{q}$  are determined for a given invariant mass  $M_{\Lambda p}$  through

$$|\vec{q}| = \sqrt{2\mu_{\Lambda p}(M_{\Lambda p} - m_p - m_{\Lambda})}, \quad (34)$$

and

$$|\vec{Q}| = \sqrt{2\mu_{(\Lambda+p)B}(m_{K^-} + 2m_p - B_{l_1 l_2} - M_{\Lambda p})}. \quad (35)$$

The angle  $\theta_{Qq}$  between  $\vec{Q}$  and  $\vec{q}$  is constrained such that  $-1 \leq \cos\theta_{p\Lambda} \leq -0.8$ . Calculated invariant mass distribution along with the corresponding measured FINUDA distribution [1] are shown in Fig. 6. We observe that, compared to the mass of  $K^- pp$  in the free state (2370 MeV) the calculated distribution is down-shifted in mass by about 50 MeV due to proton binding in  $^{12}\text{C}$ . The measured mass distribution, however, is still below this by an additional 70 MeV or so. This, incidentally, is around the reported calculated binding energy in the literature of the “ $K^- pp$ ” module taking  $\Lambda(1405)$  mass 27 MeV below  $K^- N$  threshold.

The range of the values of  $q$  and  $Q$  for  $2290 \leq M_{p\Lambda} \leq 2320$  MeV, (which covers the calculated distribution) are 520-490 and 27-320 MeV/c respectively. This says that the values of  $q$  are large and do not vary much, hence  $g(q)$  is not likely to influence the shape of the mass distribution. Its shape would be mainly determined by the nuclear wave function through  $G(Q)$  and the factor  $Q$  in the phase space.

If we include in the kinematics of our calculations an additional binding energy of 70 MeV in the initial system, then, we find that the peak position in the calculated mass distribution (not plotted here), of course, comes near to the peak position of the measured distribution, but the shape of the calculated distribution turns out much sharper than the experimental one. The calculated  $\Lambda$  momentum distribution with the additional binding also gets shifted towards lower momenta. This then spoils the agreement of the calculated results with the experiments shown above in Fig. 5 without any “ $K^- pp$ ” binding. The angular correlation between  $\Lambda$  and proton, however, remains unchanged.



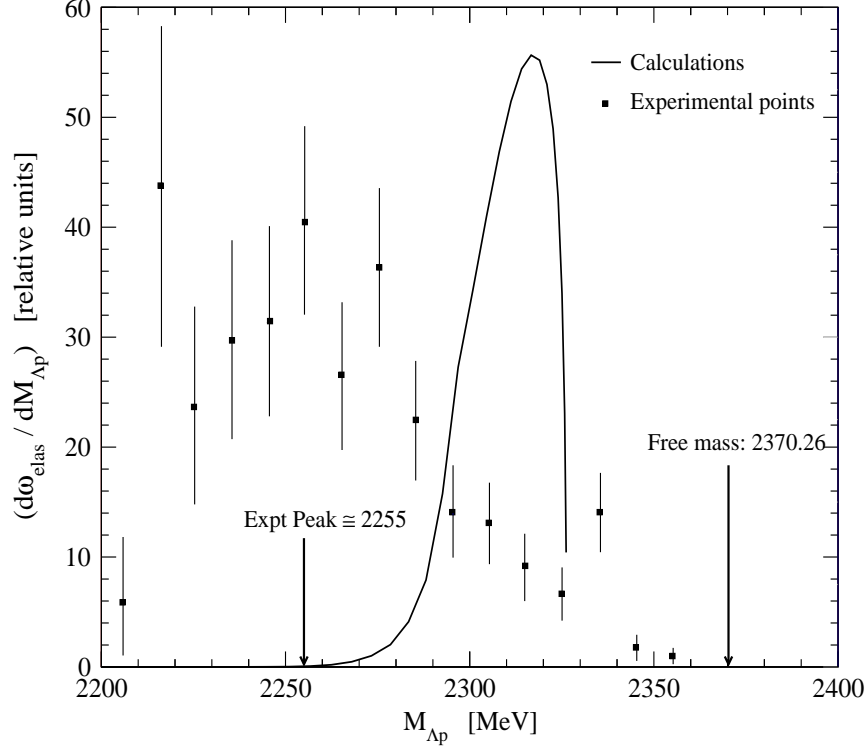


FIG. 6: Invariant mass distribution of  $\Lambda$  and  $p$  along with FINUDA measurements.  $-1 \leq \cos \theta_{p\Lambda} \leq -0.8$ .

### 5. Conclusion

In the two-nucleon  $K^-$  absorption model, with only elastic scattering of  $p$  and  $\Lambda$  included in the final state, the measured  $\Lambda$ - $p$  angular correlation distribution is reproduced well, and the momentum spectrum of  $\Lambda$ 's to a reasonable extent without introducing any additional binding of the “ $K^- pp$ ” module. The calculated invariant  $\Lambda$ - $p$  mass distribution, however, peaks around 70 MeV higher than the measured one. Attributing this shift to the additional binding of the “ $K^- pp$ ” module, the calculations including this binding in kinematics, obviously, reproduce the peak position of the measured mass distribution, but the shape of the distribution remains very narrow. It also spoils the agreement with the  $\Lambda$  momentum distribution achieved without including any “ $K^- pp$ ” binding. Thus, in an overall conclusion it seems that the observed invariant mass distribution in the  $(K^-, p\Lambda)$  reaction does not correspond to the peak predicted in this Section with only elastic scattering included in the FSI.



## B. Knock-out scattering

The knock-out scattering means that the proton or  $\Lambda$ , emanating from vertex I, encounters a hard collision with a nucleon in the residual nucleus and knocks it out (Fig. 2b). This collision alters significantly the momentum distribution of the striking particle. To calculate the knock-out contribution we recollect that, as discussed in the earlier Section,  $p$  and  $\Lambda$  move back to back at vertex I and the vertex itself is localized on the surface of the target nucleus. Because of this only one particle goes into the nucleus, the other one moves out. For such trajectories, as discussed earlier in Section A(2) for distorted waves in elastic scattering, here too the contribution of  $p$  and  $\Lambda$  to KO FSI can be included by considering the passage of only one of the two particles, but through the whole nucleus. This can be reasonably correct if the elastic scattering parameters for  $pN$  and  $\Lambda$ - $N$  systems at intermediate energies are not much different. Considering that it is so, in the following we calculate the KO contribution induced by the proton.

Let  $f(\vec{p}_p)$  describe the momentum distribution of the proton when it incidents on the vertex II, where  $\vec{p}_p'$  is the momentum of the proton at the time of leaving the vertex I. The altered momentum of this proton after the KO scattering is denoted by  $\vec{p}_p$ . The proton with this momentum along with the  $\Lambda$  are detected in the experiment. The knocked-out nucleon from the nucleus is not seen. The probability for this “inclusive” process is determined by the product of  $f(\vec{p}_p')$  and the proton induced inclusive single nucleon knock-out cross section as

$$d\omega_{KO} = f(\vec{p}_p') \frac{\sigma_{KO}(\vec{p}_p, \vec{p}_p')}{\sigma_T^{pB}(p_p')}, \quad (36)$$

where  $\sigma_T^{pB}(p_p')$  is the total proton-nucleus cross section at the momentum  $|\vec{p}_p'|$ . Momentum  $|\vec{p}_p'|$  is given in terms of the variables at the first vertex. In terms of  $\vec{p}_\Lambda$  it is given by

$$|\vec{p}_p'| = \mu_{p'B} \left[ \frac{-|\vec{p}_\Lambda| \cos(\theta_{\Lambda p'})}{M_B} + \left[ \left( \frac{|\vec{p}_\Lambda| \cos(\theta_{\Lambda p'})}{M_B} \right)^2 - \left( \frac{2}{\mu_{pB}} \right) \left( \frac{m_\Lambda}{\mu_{\Lambda B}} T_\Lambda - M \right) \right]^{1/2} \right], \quad (37)$$

where all the notations are self explanatory.  $T_x$  represents the kinetic energy of the particle  $x$ .  $M = m_K + M_A - m_p - m_\Lambda - M_B$ . Function  $f(\vec{p}_p')$  is obtained from Eq. (31), by first writing the phase space  $[PS]$  for  $\vec{p}_\Lambda$  as,

$$[PS] = \frac{m_\Lambda M_B}{(2\pi)^5} \frac{|\vec{p}_p'| |\vec{p}_\Lambda|^2}{(m_\Lambda + M_B) |\vec{p}_\Lambda| + |\vec{p}_p'| m_\Lambda \cos(\theta_{\Lambda p'})} d\vec{p}_\Lambda, \quad (38)$$



and then substituting this phase space expression in Eq. (31), and identifying  $f(\vec{p}_p')$  with  $(d\omega_{elas} / dp_p')$ . This gives

$$f(\vec{p}_p') = \left[ \frac{m_\Lambda M_B}{(2\pi)^5} \frac{|\vec{p}_p'| |\vec{p}_\Lambda|^2}{(m_\Lambda + M_B) |\vec{p}_\Lambda| + |\vec{p}_p'| m_\Lambda \cos(\theta_{\Lambda p'})} d\vec{p}_\Lambda \right] \times \left[ C |\eta_A(T_p)|^2 N_{l_1 l_2} \sum_L (l_1 l_2 00 / L 0)^2 |g_{l_1 l_2}^L(P_B)|^2 \right] \quad (39)$$

However, before we proceed further let us mention that Eq. (36) for the knock-out contribution, which has a factorization of the vertex I and II, holds under a certain approximation. More correctly, as shown in diagram 2(b) these two vertices should have been correlated in space through the proton (or lambda) propagator between them. This propagator would be a proton scattered wave between the two vertices with an outgoing boundary condition. That is, we would have between two vertices a factor like

$$\int d\vec{p} \frac{f(\vec{p}, \vec{p}')}{|\vec{p}'|^2 - |\vec{p}|^2 - 2mU + i\epsilon}, \quad (40)$$

where  $f(\vec{p}, \vec{p}')$  collectively represents all other factors.  $U$  represents the proton interaction with the medium. This integral has two parts, one originating from the principal value and another from the energy conserving  $\delta$ -function part of the propagator. Physically these two parts represent the off-shell and the on-shell scattering in the intermediate state. The on-shell part can be shown to be roughly proportional to the proton momentum, hence dominates at higher energies. The off-shell part dominates at lower energies (see for example [27]). In our case, since the energies of the proton (or lambda) are in the intermediate energy range, we have restricted ourselves to the energy conserving on-shell contribution only. This, essentially is the assumption implicit in writing Eq. (36) with the proton being described at both vertices by distorted waves.

### 1. Inclusive Knock-out Cross section

Proton induced single nucleon knock-out reaction at intermediate energies is a well studied subject experimentally as well as theoretically [21]. Using the notations given in diagram



(2b), the expression for the  $(p, pN)$  knock-out reaction is given by

$$\frac{d\sigma}{d\vec{p}_p} = \frac{1}{(2\pi)^5} \frac{1}{v'_p} \sum_n \int d\vec{p}_N d\vec{Q}_R \delta(T'_p - T_p - T_N - T_R - E_n^*) \times \delta(\vec{p}'_p - \vec{p}_p - \vec{p}_N - \vec{Q}_R) \sum \bar{|T_n(\vec{p}'_p, B \rightarrow \vec{p}_p, \vec{p}_N, \vec{Q}_R, X_n)|^2}, \quad (41)$$

where  $\sum$  denotes the average and sum over the spins in the initial and final states respectively.  $\vec{Q}_R$  is the momentum of the recoiling nucleus.  $X_n$  and  $E_n^*$  denote its intrinsic excitation and the excitation energy respectively. To evaluate this expression, first we integrate over  $\vec{p}_N$  and utilize the momentum conserving delta function, giving

$$\frac{d\sigma}{d\vec{p}_p} = \frac{1}{(2\pi)^5} \frac{1}{v'_p} \sum_n \int d\vec{Q}_R \delta(T'_p - T_p - T_N - T_R - E_n^*) \times \sum \bar{|T_n(\vec{p}'_p, B \rightarrow \vec{p}_p, \vec{p}_N, \vec{Q}_R, X_n)|^2}, \quad (42)$$

with  $\vec{p}_N = \vec{p}'_p - \vec{p}_p - \vec{Q}_R = \vec{q} - \vec{Q}_R$ , where  $\vec{q} = \vec{p}'_p - \vec{p}_p$  is the momentum transfer from the incident proton.

The transition matrix  $T_n$  in above describes the T-matrix for the knock-out of a nucleon from the nucleus B and leaving the residual nucleus in a one-hole excited state denoted by 'n'. It is given by

$$T_n(\vec{p}'_p, B \rightarrow \vec{p}_p, \vec{p}_N, X_n) = \langle p, \vec{p}_p; N, \vec{p}_N; X_n, \vec{Q}_R | t_{p'N \rightarrow pN}(\epsilon) | p', \vec{p}'_p; B \rangle, \quad (43)$$

where  $B$  and  $X_n$  denote the nuclear wave functions in the initial and final states respectively.  $t_{p'N \rightarrow pN}$  is the  $N$ - $N$  scattering amplitude. This amplitude is half off-shell if the distortion of the continuum nucleons is ignored and becomes fully off-shell if the distortions are included. However, at the energies of concern to us, the off-shell effects are known not to be significant. Hence, normally the  $N$ - $N$  t-matrix here is taken on-shell and the energy,  $\epsilon$  at which it is evaluated is taken corresponding to the incident momentum  $\vec{p}'_p$ . The  $t_{NN}$  itself is related to the  $N$ - $N$  cross section in the centre of mass through

$$\frac{d\sigma}{d\Omega} = \frac{m^2/4}{(2\pi)^2} \frac{|\vec{\kappa}_f|}{|\vec{\kappa}_i|} \bar{\Sigma} |\langle \vec{\kappa}_f | t_{NN}(\epsilon) | \vec{\kappa}_i \rangle|^2, \quad (44)$$

where  $\vec{\kappa}_x$  is the  $N$ - $N$  momentum in its centre of mass, and  $m$  is the nucleon mass.

The sum over 'n' in Eq. (42) means the sum over the excited states in the recoiling nucleus consistent with the momentum conservation. Since the reaction mechanism involves only a nucleon in the nucleus B, 'n' would have only a small spread. Therefore, in the energy



delta function in Eq. (42) we can replace, to a reasonable approximation,  $E_n^*$  by the binding energy,  $B_N$  of the knocked-out nucleon in B. This simplifies the summation over  $n$  in Eq. (42). Using closure, we can then write

$$\sum_n \bar{\sum} |T_n|^2 = \bar{\sum} \int d\xi \left| \langle p, \vec{p}_p; N, \vec{p}_N; \vec{Q}_R | t_{p'N \rightarrow pN}(\epsilon) | p', \vec{p}_p'; B \rangle \right|^2, \quad (45)$$

where  $\xi$  collectively denotes coordinates of all the spectator core nucleons in the nucleus B. To proceed further we now use a simple description of the nucleus. We write the target nucleus B wave function as a product of a single nucleon ('N') wave function in a shell with quantum numbers " $nl$ " and the core nucleus wave function  $\Phi_c(\xi)$ . With this Eq. (45) reduces to

$$\sum_n \bar{\sum} |T_n|^2 = \bar{\sum} \left| \langle p, \vec{p}_p; N, \vec{p}_N; \vec{Q}_R | t_{p'N \rightarrow pN}(\epsilon) | p', \vec{p}_p'; \phi_{nl}(N) \rangle \right|^2, \quad (46)$$

with

$$\bar{\sum} = \frac{1}{4} \frac{S(l)}{(2l+1)} \sum_{m_l} \sum_{\text{nucleon-spins}}, \quad (47)$$

where  $S(l)$  is the nucleon spectroscopic factor. In the present simplified description of the nuclear wave function, it is equal to the number of nucleons in the shell " $nl$ ". For the bound nucleon we use the momentum space representation,  $\phi_{nl}(\vec{p}_N')$ , where  $\vec{p}_N'$  from the momentum conservation at the  $\langle t_{p'N \rightarrow pN}(\epsilon) \rangle$  vertex and that following Eq. (42) equals to,  $-\vec{Q}_R$ . With this identification Eq. (46) then factorizes as

$$\begin{aligned} \sum_n \bar{\sum} |T_n|^2 &= \left[ \bar{\sum}_{\sigma's} \left| \langle \sigma_p, \vec{p}_p; \sigma_N, \vec{p}_N | t_{pN}(\epsilon) | \sigma_p', \vec{p}_p'; \sigma_N', -\vec{Q}_R \rangle \right|^2 \right] \\ &\times \left[ \frac{1}{4} \frac{S(l)}{2l+1} \sum_{m_l} |\phi_{nlm_l}(-\vec{Q}_R)|^2 \right]. \end{aligned} \quad (48)$$

The single nucleon knock-out cross section expression (Eq. (42)) subsequently becomes

$$\begin{aligned} \frac{d\sigma}{dp_p} &= \frac{1}{(2\pi)^5} \frac{1}{v_p'} \int d\vec{Q}_R \delta(T_p' - T_p - T_N - T_R - B_N) \\ &\times \left[ \bar{\sum}_{\sigma's} \left| \langle \sigma_p, \vec{p}_p; \sigma_N, \vec{p}_N | t_{pN}(\epsilon) | \sigma_p', \vec{p}_p'; \sigma_N', -\vec{Q}_R \rangle \right|^2 \right] \\ &\times \left[ \frac{1}{4} \frac{S(l)}{2l+1} \sum_{m_l} |\phi_{nlm_l}(-\vec{Q}_R)|^2 \right]. \end{aligned} \quad (49)$$



To obtain the expression for the inclusive cross section we still need to integrate this expression over  $\vec{Q}_R$ . Following Ref. [22] we use the energy delta function to remove angle integration, and with some algebraic manipulations obtain

$$\begin{aligned} \int d\vec{Q}_R \delta(T'_p - T_p - T_N - T_R - B_N) \left[ \frac{S(l)}{2l+1} \sum_{ml} |\phi_{nlm_l}(-\vec{Q}_R)|^2 \right] \\ = S(l) \frac{m}{2q} \int_{Q_R^{min}}^{\infty} Q_R dQ_R |\phi_{nl}(Q_R)|^2. \end{aligned} \quad (50)$$

Substituting this in Eq. (49) above, and also writing  $\sum_{\sigma's} |\langle t_{pN} \rangle|^2$  in terms of the elementary  $N$ - $N$  differential cross section (Eq. (44)) we get

$$\frac{d\sigma}{d\vec{p}_p} = \left[ \frac{2}{qp'_p} \right] \left[ \frac{d\sigma}{d\Omega}(\epsilon) \right]_{cm}^{pN} \left[ S(l) \int_{Q_R^{min}}^{\infty} Q_R dQ_R \left| \frac{1}{(2\pi)^{3/2}} \phi_{nl}(Q_R) \right|^2 \right]. \quad (51)$$

Here  $Q_R^{min}$  is that minimum momentum which a nucleon of binding energy  $B_N$  must have in the nucleus for the scattered proton to be observed at a scattering angle  $\theta$  with a momentum  $|\vec{p}_p|$ . Its value is given by

$$Q_R^{min} = \frac{[p_p^2 - p'_p p_p \cos(\theta) + m B_N]}{[p_{p'}^2 - p'_p p_p \cos(\theta) + m B_N]^{1/2}}. \quad (52)$$

Eq. (51) for the knock-out cross section assumes that the incoming proton and the outgoing nucleons do not suffer any additional scattering except the hard knock-out collision. This additional scattering, however, can be incorporated in the formalism by replacing the plane wave description of the continuum nucleons by the “distorted waves”, which would be solutions of the wave equation with appropriate optical potentials in it. Several studies of the distortion effect in the knock-out reaction have been carried out in the literature and it has been found that in the energy range of nucleons of interest to us here, the effect of distortion is mainly absorptive. The dispersive effect is very small. The absorption factor for  $^{12}\text{C}(p, 2p)^{11}\text{B}$  reaction at 160 MeV beam energy, for example, in Ref. [23] is found to be around 0.5.

Finally, before closing this Section we determine the extent of accuracy to which the expression in Eq. (51) describes the measured inclusive proton induced single nucleon knock-out cross section. We calculate the inclusive cross sections at 160 MeV beam energy for  $^{12}\text{C}$  and compare them with the measured  $(p, p')$  ones at the same beam energy [13]. The calculated results are summed over the knocked-out nucleon (including both neutron and



proton) from  $1s$  and  $1p$  shells. The single nucleon binding energies for them are taken from Ref. [19]. The nucleon-nucleon differential cross section in the centre-of-mass required in the calculations are taken from the analytic form given in Ref. [24], i.e.

$$\frac{d^2\sigma}{d\Omega dT} = \left[ 1.9 + \frac{230}{T} + \frac{4850}{T^2} \right] (1 + 0.1 \cos^2 \theta), \quad (53)$$

where the cross section is in mb and energy (kinetic),  $T$  in MeV. This form is in good agreement with the energy dependence of the observed cross sections for the range  $20 \leq T \leq 200$  MeV.

The bound nucleon wave function is described by the oscillator potential form with the length parameter,  $b = 1.67$  fm. The spectroscopic factor,  $S(l)$  is taken equal to the number of nucleons (neutrons+protons) in the orbital  $nl$ .

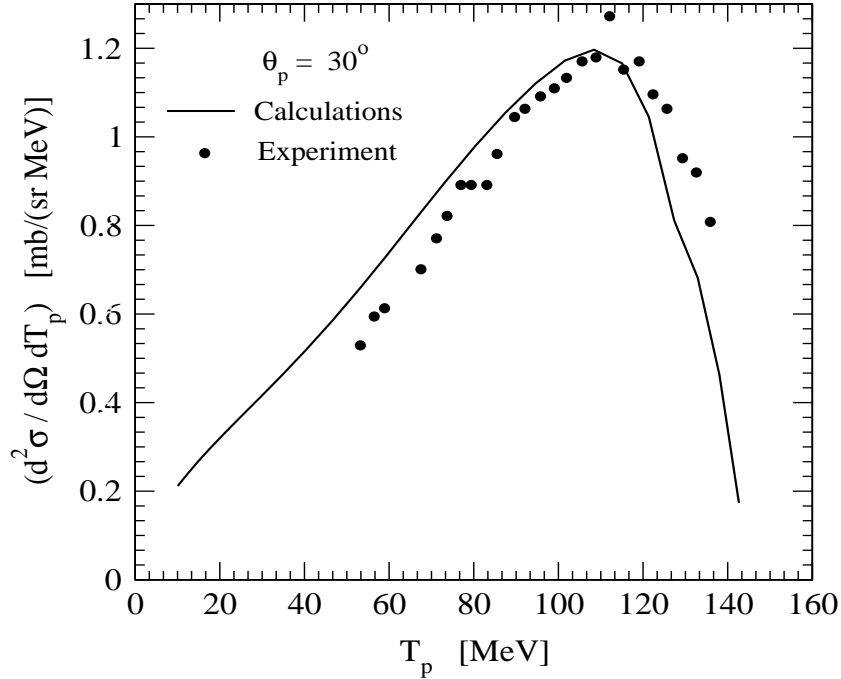


FIG. 7: Calculated energy spectrum of a 160 MeV incident proton on  $^{12}\text{C}$  after a single nucleon knock-out scattering from the nucleus along with the experimental points at the same energy [13].

With these inputs and the distortion factor equal to 0.5 (as discussed above), the calculated energy spectrum for the proton going at  $30^\circ$ , for example, in the lab. frame along with the experimental cross sections is shown in Fig. 7. As we see, the agreement between them, both in shape and magnitude, is very good. This validates the accuracy of Eq. (51) for the



description of the inclusive knock-out channel and gives confidence for its use in calculations of the  $(K^-, p\Lambda)$  reaction.

## 2. Results

The final expression for calculating the knock-out contribution to the  $K^-$  absorption probability is obtained by substituting Eq. (51) for  $\sigma_{KO}(\vec{p}_p, \vec{p}'_p)$  in Eq. (36). We get

$$d\omega_{KO} = [dp_\Lambda \, dp_p] f(\vec{p}_p) \times \frac{1}{\sigma_T^{pB}(T_{p'})} \left[ \frac{2}{qp'_p} \right] \left[ \frac{d\sigma}{d\Omega}(\epsilon) \right]_{cm}^{pN} \times \left[ S(l) \int_{Q_R^{min}}^{\infty} Q_R \, dQ_R \left| \frac{1}{(2\pi)^{3/2}} \phi_{nl}(Q_R) \right|^2 \right], \quad (54)$$

where  $f(\vec{p}_p)$  is given by Eq. (39). As in the case of “elastic scattering” we present here calculated results for the target nucleus  $^{12}\text{C}$ . The results are the probabilities summed over two proton hole states in various pairs of  $(n_1 l_1; n_2 l_2)$  shell model orbitals at vertex I and, for each of these pairs, summed over various one nucleon  $nl$  orbitals in nucleus  $B$  at the knock-out vertex II. Since in the final state after knock-out we do not detect the knocked out nucleon, we use the spectroscopic factor,  $S(l)$  summed over both, the neutrons and protons. The radial part of the bound state wave functions, as discussed in the last Section, is taken for the oscillator potential. The differential scattering cross section for  $p$ - $N$  is described by Eq. (53) with energy taken corresponding to momentum  $\vec{p}'_p$  of the proton incident at the vertex II (Fig. 2b). Required  $\sigma_T$  for proton on nucleus  $B$  at energies corresponding to different proton momentum,  $|p'_p|$  is taken from Ref. [25]. This cross section, of course, does not vary significantly over the  $p'$  energy range of interest here.

The physical effect of knock-out scattering at vertex II is to reduce the energy of the proton  $p'$  and deflect it from its direction of incidence. The amount of these changes, as can be seen from the experimental results on inclusive  $(p, p')$  reaction at 160 MeV in Ref. [13], are about 30 MeV and above for the energy reduction and about  $30^\circ$  and above for the deflection. Immediate consequence of these numbers would be that the angular correlation between  $p$  and  $\Lambda$  shown in Fig. 4, coming from vertex I, will be widened significantly and the energy spectrum of  $p$  and  $\Lambda$ , shown in Fig. 5, will be shifted towards lower energies. Both these effects will, therefore, spoil the agreement shown in these figures (Figs. 4-5) between the calculated results from vertex I and the corresponding FINUDA measurements. To get



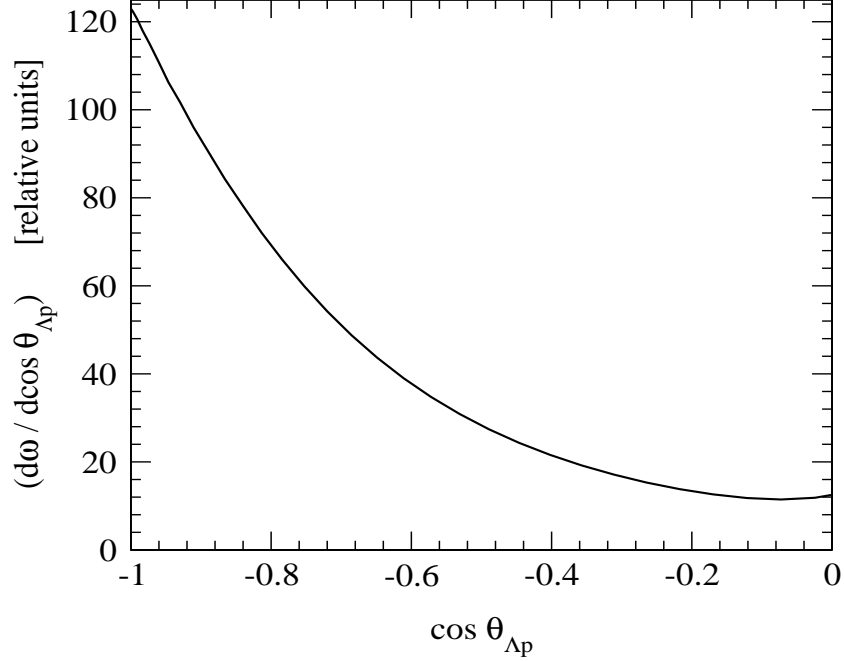


FIG. 8: Angular distribution of an incident proton after a single nucleon knock-out scattering on vertex II.

a quantitative idea about the extent of deflection the vertex II may introduce in the proton,  $p'$ , in Fig. 8 we show its angular distribution relative to the  $\Lambda$  motion after being scattered from the vertex II. Initially the  $p'$  is taken to move at  $180^\circ$  w.r.t.  $\Lambda$  with energy as fixed at the vertex I, including the spread due to Fermi motion. Without the knock-out scattering, this distribution will be just a point at  $\cos(\theta_{p\Lambda})=-1$  in this figure. Due to scattering this point gets a significant spread, as we see in this figure. Calculated results use Eq. (54) and are integrated over the energy spread of  $p'$ .

The consequence of above is expected to be a significant modification in the invariant mass distribution of the  $p$  and  $\Lambda$ . However, before we show these results we may mention that, because of various sums, integrals and constrain checks on kinematic variables, the calculations are very involved and tedious. Therefore, to keep the calculations somewhat simpler and physically transparent we have put some constraints in the calculations without, of course, losing any essence of the physics of the results. We have seen earlier in the calculations on vertex I that the  $p$  and  $\Lambda$  from it emerge mainly back-to-back with a very small cone angle. We have, therefore, done the vertex II calculations with  $\theta_{p\Lambda} = 180^\circ$  only. The



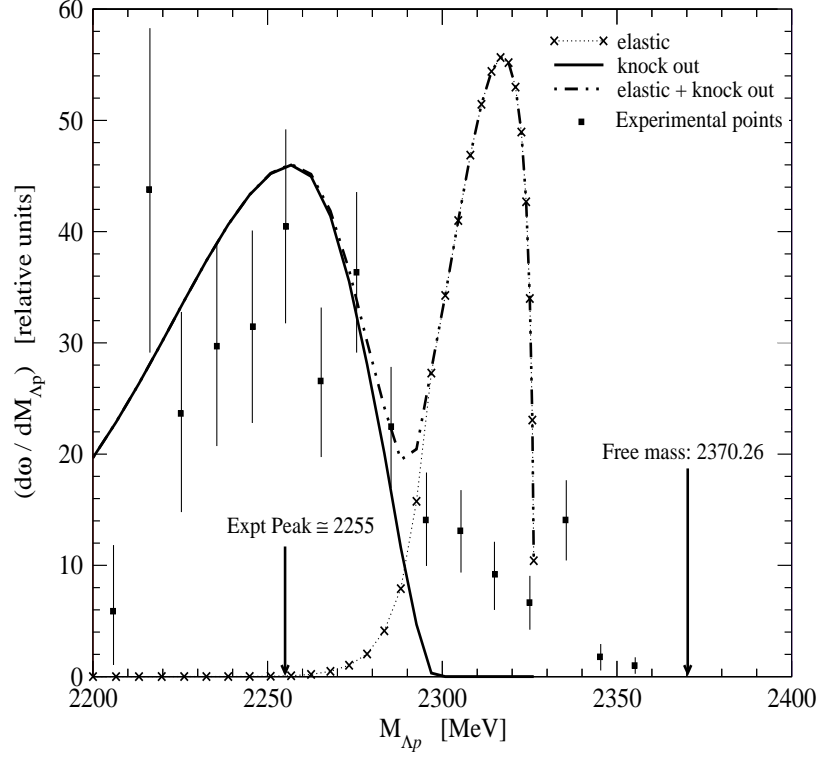


FIG. 9: Invariant  $p\Lambda$  mass distribution from both the vertices along with the experimental points [1].

energy variation of the  $p$  and  $\Lambda$  due to Fermi motion of the absorbing protons in the nucleus  $A$ , however, has been kept intact. With this, in Fig. 9 we show the calculated invariant mass distribution of  $p\Lambda$  after knock-out scattering along with the FINUDA measurements [1]. It is extraordinary to see that the calculated mass distribution totally agrees with the measured ones. They agree in mass shift as well as in the shape of the distribution. This is the same observation as reported in Ref. [12].

However, to get the complete  $p\Lambda$  invariant mass distribution we need to add to above the contribution from the “elastic scattering” FSI corresponding to vertex I (Fig. 2a). Therefore, in Fig. 9 we also show the  $p\Lambda$  invariant mass distribution due to vertex I, and the sum of the “elastic” and “knock-out” contributions. The summed distribution obviously has two peaks, one corresponding to “elastic scattering” FSI and another to the “single nucleon knock-out” FSI. This is similar to the inclusive inelastic spectrum normally seen experimentally in  $(p, p')$  or  $(e, e')$  scattering on any nucleus at “intermediate energies” [13]. Unusual thing following  $K^-$  absorption seen here is that the peak corresponding to “elastic



scattering” seems to be missing in the FINUDA data. This is intriguing.

### 3. *Conclusions*

We summarize our observations for the Vertex II as,

1. The calculated invariant  $p$ - $\Lambda$  mass distribution totally reproduces the experimentally observed distribution. This is in line with the finding in Ref. [12].
2. Though we have not shown the full calculations for the inclusive energy spectra for the proton or lambda and angular correlation between them, we believe that due to large deflection and energy shift by the single-nucleon knock-out scattering the agreement seen in Figs. 4-5 between the observed and calculated angular correlation between the  $p$  and  $\Lambda$  and the inclusive  $p$  and  $\Lambda$  energy spectra using only the vertex I will be spoiled considerably. We have not calculated these spectra fully because, due to several integrations over various kinematic variables, they are very long and involved.

## IV. SUMMARY AND FINAL CONCLUSIONS

We have calculated the inclusive differential absorption probability for  $K^-$  at rest in  $^{12}\text{C}$  nucleus for the  $p\Lambda$  exit channel. The  $K^-$  is assumed to be absorbed on a pair of protons in the nucleus. The final state interaction in the reaction includes the elastic scattering of  $p$  and  $\Lambda$  in the final state and the single nucleon knock-out from the recoiling nucleus. The calculated invariant  $p$ - $\Lambda$  mass distribution shows two peaks, one due to elastic scattering and another due to knock-out channel. The latter peak overlaps in position and width with the peak observed in the FINUDA measurements. The peak corresponding to elastic scattering is not seen in the experiments.

Measured angular correlation between  $p$  and  $\Lambda$  and their inclusive energy distribution agree with the corresponding calculated results including only the elastic scattering in the final state. Inclusion of the knock-out channel is likely to spoil this distribution.

Thus, finally, we may conclude that, seen in isolation, the experimentally observed shift in the invariant  $p$ - $\Lambda$  mass distribution could be interpreted as due to single nucleon knock-out final state interaction. But, if we include other results, like the absence of elastic scattering



peak in experiments, full agreement of the calculated  $p$ - $\Lambda$  angular correlation and their inclusive spectra using only vertex I with the corresponding measurements, the situation becomes quite a bit confusing.

As a final comment in the present work on the “ $K^- p p$ ” cluster interpretation of the observed downshift of about 100 MeV in the FINUDA measurements of the  $\Lambda p$  invariant mass compared to its free value, the knock-out reaction in the final state seems to be a definitive alternative for this shift. Only discomfiture in this conclusion comes from the absence of the “elastic scattering” peak (Fig. 9) in the observed invariant mass distribution in the FINUDA measurements. This absence can not be attributed to the cut off of the  $\Lambda$  hyperons below 300 MeV/c momentum in the FINUDA spectrometer as these momenta in the “elastic scattering” peak are above 400 MeV/c.

Availability of absolute measurements may help to understand the ( $K^-$ ,  $p \Lambda$ ) reaction better.

## V. ACKNOWLEDGEMENTS

The authors are extremely grateful to Dr. Neelima Kelkar and Dr. Kanchan Khemchandani for many useful suggestions and their comments on the presentation of the work. This work was initiated sometime back when BKJ visited the Institute of Particle and Nuclear Studies, KEK, Japan. He thanks Prof. Shunzo Kumano and other members of the Institute for many useful academic discussions and their hospitality during the stay. The work was done under the financial grant from the Department of Science and Technology, Govt. of India.

- 
- [1] M. Agnello *et al.*, Phys. Rev. Lett. **94**, 212303 (2005).
  - [2] H. Fujioka *et al.*, Nucl. Phys. **A827**, 303c (2009).
  - [3] T. Yamazaki *et al.*, Proceedings of the International Conference on Exotic Atoms and Related Topics and International Conference on Low Energy Antiproton Physics (EXA/LEAP 2008), Vienna, Austria, 2008; arXiv:0810.5182v1.
  - [4] N. Kaiser, P. B. Siegel, and W. Weise, Nucl. Phys. **A594**, 325 (1995).



- [5] B. Krippa, Phys. Rev. C **58**, 1333 (1998); E. Oset and A. Ramos, Nucl. Phys. **A635**, 99 (1998); J. A. Oller and U. G. Meißner, Phys. Lett. **B500**, 263 (2001); M. F. M. Lutz and E. Kolomeitsev, Nucl. Phys. **A700**, 193 (2002).
- [6] C. Amsler *et al.* (Particle Data Group), Phys. Lett. **B667**, 1 (2008) (<http://pdg.lbl.gov>).
- [7] T. Hyodo and W. Weise, Phys. Rev C **77**, 035204 (2008).
- [8] I. Zychor *et al.*, Phys. Lett. **B660**, 167 (2008).
- [9] Y. Akaishi and T. Yamazaki, Phys. Rev. C **65**, 044005 (2002).
- [10] A. Dote, T. Hyodo, and W. Weise, Nucl. Phys. **A804**, 197 (2008); arXiv:0802.0238.
- [11] N. V. Shevchenko, A. Gal, and J. Mares, Phys. Rev. Lett. **98**, 082301 (2007); J. Revai, Phys. Rev. C **76**, 044004 (2007).
- [12] V. K. Magas, E. Oset, A. Ramos, and H. Toki, Phys. Rev. C **74**, 025206 (2006).
- [13] N. S. Wall and P. R. Roos, Phys. Rev. C **150**, 811 (1966).
- [14] G. E. Brown, *Unified Theory of Nuclear Models and Forces* (North-Holland Pub., 1967), p. 201.
- [15] R. Jastrow, Phys. Rev. **98**, 1479 (1955).
- [16] Daphne F. Jackson, *Nuclear Reactions* (Methuen & Co. Ltd., London, 1970), Ch. 3.10.
- [17] A. G. Sitenko, *Theory of Nuclear Reactions* (World Scientific Publishing, 1990), p. 550-555.
- [18] L. R. Suelzle, M. R. Yearian, and Hall Crannell, Phys. Rev. **162**, 992 (1967); B. K. Jain, Phys. Rev. C **27**, 794 (1983).
- [19] H. Tyren, S. Kullander, O. Sundbag, R. Ramchandran, P. Isaccson, and T. Berggren, Nucl. Phys. **79**, 321 (1966); W. D. Simpson *et al.*, Nucl. Phys. **A140**, 201 (1970).
- [20] H. Fujioka, Graduate Study Report, Nagae Laboratory, Department of Physics, University of Tokyo, 2005, p. 130 (unpublished).
- [21] G. Jacob and Th. A. J. Maris, Nucl. Phys. **31**, 139 (1962); Rev. Mod. Phys. **38**, 121 (1966); T. Berggren and H. Tyren, Ann. Rev. Nucl. Sci. **16**, 153 (1966); Daphne F. Jackson, Adv. Nucl. Phys. **4**, 1 (1971); R. Shanta and B. K. Jain, Nucl. Phys. **B175**, 417 (1971); R.E. Chrien *et al.*, Phys. Rev. C **21**, 1014 (1980); J. S. O'Connell *et al.*, *ibid* **35**, 1063 (1987).
- [22] Peter A. Wolff, Phys. Rev. **87**, 434 (1952).
- [23] F. R. Kroll and N. S. Wall, Phys. Rev. C **1**, 138 (1970).
- [24] K. F. Riley, Nucl. Phys. **13**, 407 (1959).
- [25] S. Barshay, C. B. Dover, and J. P. Vary, Phys. Rev. C **11**, 360 (1975); R.M. de Vries and J.



- C. Peng, Phys. Rev. C **22**, 1055 (1980); P. Renberg *et al.*, Nucl. Phys. **A183**, 81 (1972).
- [26] G. Backenstoss *et al.*, Nucl. Phys. **73**, 189 (1974).
- [27] N. J. Upadhyay, K. P. Khemchandani, B. K. Jain, and N. G. Kelkar, Phys. Rev. C **75**, 054002 (2007); N. J. Upadhyay, N. G. Kelkar, and B. K. Jain, Nucl. Phys. **A824**, 17 (2009).
- [28] K. Aslam and J. R. Rook, Nucl. Phys. **B20**, 159 (1970).